

## EXPERIMENTAL STUDY OF ENHANCED LAMINAR NATURAL CONVECTION HEAT TRANSFER FROM STAGGERED CYLINDERS ARRANGED IN AN INCLINED ARRAY

Yasin K. Salman & Khalid G. Muhammed

Research Scholar, Department of Energy Engineering University of Baghdad, Iraq

Received: 18 Jun 2019

Accepted: 08 Jul 2019

Published: 24 Jul 2019

### ABSTRACT

An experimental investigation to a laminar natural convection heat transfer from an inclined array of the circular cylinder was presented in this study. Inclined cylinders were subjected to constant heat flux and were arranged in staggered in a bank. The apparatus of investigation consists of five identical in dimension cylinders and the staggered arrangement with longitudinal (flow direction) and traversing spacing distances of  $5 D$  and  $2.5 D$ , respectively. The study cover  $Ra_{L,D}$  range varies from 50600 to 108000 and five inclination angles  $0^\circ$ ,  $30^\circ$ ,  $45^\circ$ ,  $60^\circ$  and  $90^\circ$  (vertical). The local surface temperature  $T_x$ , local heat transfer coefficient  $h_x$  and average heat transfer coefficient  $h_L$  variation with cylinder length are presented for all bank inclination angles. Variations of average Nusselt number  $Nu_{L,D}$  with the Rayleigh number  $Ra_{L,D}$  are also correlated for all array inclination angles and for each individual cylinder in the array. With exception of the vertical orientation, results show an increasing rate of heat transfer from two cylinders located in the upper corners of the array in comparison with two cylinders located in the lower corners cylinders and the cylinder located at arrays center. The natural convection current interference shows no effect on the two lower corner cylinders and array central cylinder. This process enhancement shows a significant heat transfer decreasing rate for array inclination angle between horizontal to  $30^\circ$  ranges than with a constant rate between  $30^\circ$  and  $60^\circ$  and another decreasing rate as the bundle moves toward a vertical orientation which reveals the lowest heat transfer rate. In general, for each individual cylinder in bank, heat transfer process improved as the bank moves from vertical to horizontal. A good agreement with a previous work results obtained for single horizontal cylinder but a contradictory agreement with a previous work results obtained for a single vertical cylinder. Comparison for the upper cylinders in the bank with available experimental and analytical previous work reveals a good agreement.

**KEYWORDS:** Heat Transfer, Natural Convection, Inclined Cylinders, Staggered Array

### INTRODUCTION

A convection heat transfer process is a process whose rate is directly affected by the fluid motion. Energy transfer between the solid surface and surrounding fluid can take place under the effect of external force and also under the effect of different in fluid densities caused by the local heating and cooling occurs in the gravity field. External flow situation makes natural convection solution analytically difficult and the solution required a number of a simplifying assumption. Therefore, studying natural convection heat transfer required knowledge about the transport mechanism of the laws governing the fluid flow and heat transfer processes. Natural convection heat transfer investigation and governing empirical formulas depend mostly on the experimental foundation. The flow visual observation (flow visualization) is usually supported with the experimental study to obtain the complete images for the fluid flow situation accompanied with

the heat transfer process.

Heat transfer by laminar natural convection from inclined circular cylinder array or from a single inclined circular cylinder have been used in many industrial applications such as in the cooling of many electronic equipment, safety criteria of nuclear reactor devices, conversion of the ocean thermal energy and the extraction of heat from solar thermal storage solar thermal storage devices. Natural convection heat transfer from the outside surfaces of inclined cylinders investigated experimentally and theoretically in many studies for both the constant temperature and constant heat flux situations. Empirical correlation equations presented by **Morgan [1]** and others have been focused mainly on the time-averaged Nusselt number. Experiments executed on a four aluminum cylinders bank by **Oosthuizen [2]** to evaluate the average heat transfer coefficient from inclined cylinders to air. Bank inclinations cover a complete range from horizontal to vertical and  $Gr_d$  range varied from 40000 to 90000. The cooling time was of the order of 300s which was considered short enough for the calculated heat transfer to be effectively equal to that applicable to the steady-state heat transfer. **Al-Arbi and Salman [3]** studied experimentally heat transfer by laminar natural convection from the outside surface of a copper cylinder subjected to a uniform surface heat flux. A nickel electroplated cylinder has a length equal to 950 mm, outside diameter equal to 38 mm and wall thickness equal to 1 mm and experiments performed for five different cylinder orientations,  $0^\circ$  (horizontal),  $30^\circ$ ,  $45^\circ$ ,  $60^\circ$  and  $90^\circ$  (vertical). An investigation concluded that for the same heat flux, both the local and the average Nusselt numbers increase as the cylinder inclination angle moves from the vertical position to horizontal. The minimum rate of heat transfer occurs in the vertical position while the maximum rate of heat transfer value obtained in the horizontal position. The limit of the laminar region stated as  $Gr_x \cdot Pr$ , increases with the cylinder orientation from the vertical and diminished after  $45^\circ$ ). For a cylinder subjected to constant heat flux, two empirical formulas for local and average heat transfer results are correlated to cover all cylinder orientations. **Popiel et-al [4]** investigated experimentally and analytically natural convection heat transfer to the air by from a vertical isothermal slender circular cylinder using the transient technique. The result is presented in an approximating numerical table data in a good agreement with the experimental results and reveals more accurate results than other known correlations. Conclusion for vertical isothermal circular cylinder cannot be treated as a flat plate and the free convective heat transfer rate increased as the result of a slight shift in the flow movement in the vicinity of a vertical cylinder can be a very sensitive rising column of fluid from the hot cylinder surface.

Steady-state natural convection from a vertical bank of horizontal circular cylinders was investigated by **Marsters [5]**. The study covers three cases for the number of cylinders in the bank three, five and nine and the effect of cylinder spacing distance was also presented. Natural convection heat transfer from a pair of horizontal cylinders arranged vertically was studied by **Sparrow and Niethammer [6]** experimentally. The effect of the vertical cylinder separation distance reported and the effect of the cylinder to cylinder temperature difference on the upper cylinder Nusselt number. Results reveal that the upper cylinders heat transfer rate takes a maximum value and depends upon separation distance. Result also indicated that for a small cylinders separation distance, the cylinder to cylinder temperature difference has a great effect on the Nusselt number.

**Tokura et-al [7]** performed experiments on natural convection heat transfer to air from two, three and five horizontal tubes arranged in a vertical array. Experiments concluded that buoyant flow interference for a small separating distance (less than 1 D), decreases the heat transfer rate as the result natural convection is dominated by the preceding hot tube. Heat transfer rates increases as cylinders separating distance go beyond 1 D. Heat transfer rate for the entire tubes

array was found depends on many factors such as the number of tubes in the array, tube separating distance and tube diameter. **Karvinen and Kauramaki [8]** investigated experimentally natural convection heat transfer from an array composed of four horizontal, isothermal cylinders in water. **Reymond, et-al [9]** studied natural convection heat transfer from a single and pair of identical horizontal circular cylinders aligned vertically. For Rayleigh number range from 2000000 to 6000000, investigation covers three cylinders spacing 1.5, 2 and 3 diameters. The surface circumferential temperature variations were presented to reveal the variation of heat transfer rate around the cylinder circumference. Results also reveal that the lower cylinder in the bank unaffected by the present of other cylinders in the bank. This is true for the second cylinder if the first cylinder kept unheated. The lower cylinder plume upward rising was found interacting and interferes with the upper cylinder and that is significantly affecting the cylinder heat transfer circumferential distribution and heat transfer rate. The plume oscillations affecting the cylinders heat transfer process also investigated which reveal creating an increase of the flow mixing and enhancing the overall heat transfer process. **Chouikha et-al [10]** studied experimentally natural convection heat transfer from two horizontal heated cylinders arranged in a vertical array. The effects of cylinder spacing on the heat transfer process, increasing of Rayleigh number and flow behavior around both cylinder were investigated. The study concluded that the bottom part of cylinder heat transfer rate remains the same as that of a single cylinder while the top part cylinder displayed reduced in the Nusselt number at small cylinders spacing and enhanced Nusselt numbers at large cylinders spacing. For same spacing, changing the heat flux exhibited an increase in the heat transfer rate at the top of the cylinder with increasing the Rayleigh number and this behavior is consistent with the properties of the flow field around the cylinders. Results suggested that it will be sufficiently versatile to permit investigation with an array of several cylinders [11]. An experimental investigation has been presented by **Sparrow and Boessneck [12]** to study natural convection heat transfer from an array of pair of horizontal cylinders with uniform surface temperature, in a range of Rayleigh numbers from 20000 to 200000. An investigation has found that the array orientation has enhanced the heat transfer of the top part of the cylinder. However, the range of Rayleigh numbers is very much higher than in the practical cases

The above survey shows that the natural convection heat transfer from a bank of horizontal cylinders arranged vertically in an array exist and presented in a limited reference. Heat transfer by natural convection from an inclined array of cylinders has given no attention and the present investigation was carried out as a humble contribution in this field. The experimental test runs have been arranged to study natural convection heat transfer to still air from a bank of cylinders capable to be configured either in-line or staggered. All cylinders in the array manufactured identically and subjected to a constant heat flux. Experimental test runs intended to cover heat flux range from 621.58 to 1350 W/m<sup>2</sup> while the bank will be oriented to cover the complete range from 0° (horizontal) to 90°(vertical). The cylinders arranged with traversing and longitudinal spacing are 5 D and 2.5 D, respectively.

## Nomenclature

Table 1

Symbol	Description	Unit
A <sub>s</sub>	Outside surface area of cylinder	m <sup>2</sup>
b	Separating distance ( surface to surface) between cylinders	M
C <sub>p</sub>	Specific heat	J/kg.□/
D	Diameter of cylinder	M
F	Shape factor for radiation calculation	

g	Acceleration due to gravitational	$m/s^2$
h	Heat transfer coefficient	$W/m^2 \cdot \square /$
k	Thermal conductivity	$W/m \cdot \square /$
L	Length of the cylinder	M
P	Symbol of the cylinder in the array	
q	Heat flux	$W/m^2$
q conv.	Convection heat flux	$W/m^2$
Q cond.	Heat loss by conduction	W
Q conv.	Heat loss by convection	W
Q rad.	Heat loss by radiation	W

Table 2

Q <sub>tot</sub>	Total heat input	W
S	Center to center spacing for cylinders	M
T	Temperature	$\square e$
x	Axial coordinate	M

### Greek Symbols

Table 3

$\beta$	Thermal expansion coefficient	$1/^\circ K$
$\theta$	Array orientation angle	Degree
$\mu$	Dynamic viscosity	$Kg/m \cdot s$
$\nu$	Kinematics viscosity	$m^2/s$
$\Psi$	Bank Configuration angle	Degree

### Dimensionless Group

Table 4

Gr	Grashof number	$g \beta (T_s - T_a) D^3 / \nu^2$
Nu	Nusselt number	$h \cdot D / K$
Pr	Prandtl number	$\mu \cdot C_p / K$
Ra	Rayleigh number	$Gr Pr$

### Subscript

Table 5

a	Ambient
av	Average
cond	Conduction
conv	Convection
D	Based on diameter
f	Film
L	Average , Longitudinal (flow direction for horizontal array)
rad.	Radiation
s	Surface
T	Traversing
tot	Total
x	Local

## **Experimental Apparatus and Data Reduction**

### **Experimental Apparatus**

The experimental apparatus was constructed and executed to cover the parameters range mentioned above which affect natural convection heat transfer processes from an array of staggered arranged five circular cylinders. The tested parameters comprise the heat flux subjected to cylinder surface, the array orientation, the cylinders transverse and longitudinal spacing distance and cylinders configuration in the bank. The details and cylinder configuration for the apparatus used in the present investigation is shown diagrammatically in Fig. (1) and Fig. (2), respectively. Figure (1) shows essentially detail of the experimental test rig which is consist of five identical highly polished outside surface aluminum circular cylinders ( $P_0$  to  $P_4$ ). The bundle held and supported by two identical thick square aluminum plates ( $A_1$ ,  $A_2$ ), each plate has dimensions (350 mm\*350 mm\*6 mm thickness).

The bundle with the supporting plates assembled to be an array with four suitable gripping and tied threaded steel rods (B). The array held firmly with minimum interference to the natural convection buoyant flow and to allow the array to rotate 360 degrees around a horizontal axis using the bundle holder (C) and the cylinder orientation control bolt (D). The bundle orientation was adjusted and recorded on the fixed protractor (E) which gives the bundle orientation ( $\Theta$ ).

There is another rotation axis perpendicular to the previous horizontal rotation axis represented by the bundle central cylinder  $P_1$ . This rotation serves to accommodate the bundle configuration (angle  $\Psi$ ) and it changes from  $0^\circ$  (inline) to  $45^\circ$  (staggered). The cylinder  $P_1$  stays stationary during configuration change while the other cylinders in the bundle rotate during changing the bundle configuration. The control bolt (F) is used to fix the bundle configuration. The bundle configuration angle  $\Psi$  was adjusted and recorded on another fixed protractor (G). The bundle with the bundle holder is being held firmly and stationary with the help of a vertical iron rod as a part of a heavy frame iron base (H).

The heated cylinder detail and dimensions are shown in Fig. (2). The heated cylinder consists of a highly polished aluminum circular cylinder (P) with length equal to 500 mm, outside diameter (D) equal to 29.4 mm, and cylinder thickness equal to 2 mm. Two circular Teflon (Polytetrafluoroethylene (PTFE)) pieces (I) and (J) with outside diameter equal to 29.4 mm, are machined and fitted to the lower and upper ends of the cylinder so that the Teflon pieces form a continuation to the aluminum cylinder surface on both sides. Each Teflon piece has a length of 95 mm length, and this length from both cylinder sides is sufficient to prevent restriction to natural convection buoyant flow while the bundle changes orientation. The Teflon material was selected as it is machinable and with low thermal conductivity property that will reduce the cylinder ends heat losses. The inside and outside surfaces of the cylinders are heated by means of an electric powered heater. It consists of a resistance nickel-chrome coiled wire (K) uniformly wound for a complete cylinder length to provide a constant heat flux generation per unit cylinder length. The coil is protected by an envelope of Pyrex-glass tube (L). To prevent natural convection currents inside the space between the heater glass tube and the cylinder inner surface, this space is filled with magnesium oxides (M). Magnesium oxide was selected as it has relatively high thermal conductivity and poor electrical conductance. The heater wire terminals are connected to porcelain connector pieces (N). The porcelain pieces are fitted in the holes bored centrally in the Teflon pieces at both cylinder ends and therefore keep the heater concentric in the cylinder. To assure centrality and support the heater in the cylinder three bolts are used on each cylinder side passing through the Teflon piece and gripping the porcelain piece at the heater end. The cylinder outside surface temperature is measured by sixteen 0.2 mm fiberglass covered type K thermocouples fitted along the cylinder as demonstrated in Fig. (2). The thermocouples measuring junction beads were made by fusing the ends of the two wires

together by an electric spark in a zone free of oxygen to prevent oxidation of thermocouples measuring junction. All Thermocouples were calibrated in the laboratory using the boiling point of pure chemical substances. To secure the thermocouples along the cylinder 16 holes, 1.6 mm in diameter were drilled in the cylinder wall and the outside end of each hole was chamfered by 2 mm drill to locate the measuring junction bead after passing it and whole thermocouple wire from cylinder inner surface. The beads of thermocouples secured permanently to the surface by a high-temperature Devcon adhesive. The grinding paper is used to remove the excess part of adhesive and make thermocouples spots carefully cleaned and flash with cylinder outer surface. The air laboratory ambient temperature was measured by a thermocouple located far from the effect of the hot cylinders. Each individual heater in the apparatus has been power separately using a separate electrical circuit with separate transformer and wattmeter to facilitate obtaining a simultaneously constant power supply for all the cylinders in the array. To evaluate the heat loss by conduction from the heated cylinder ends via the Teflon pieces, two thermocouples 10 mm apart were fixed in each Teflon piece as shown in Fig.(2). Knowing the thermal conductivity of Teflon and the distance between the thermocouples, the Teflon piece heat conduction loss could be evaluated. The maximum experimentally conduction heat loss value was found to vary in the range between 0.023% and 0.025% of the total input power.

The two thick aluminum gripping plates were machined by cutting cross shape groove on the plate diagonal, to enable the cylinders to change position with the help of the scale fixed on both plates by which the longitudinal and traversing spacing distance can be changed for both inline and staggered cylinders configuration in the array. This is possible by releasing the threaded bolts (B) shown in Fig. (1) and adjust the four outside cylinders either inward or outward direction related to the central cylinder  $P_1$

The experimental tests were executed in a very large volume laboratory which is very suitable for natural convection test. In spite of this precaution and to prevent any external air movement in the area adjacent to the cylinder array the entire apparatus was enclosed within a wooden frame with a transparent thick nylon shield of about 2 x 2 m horizontal dimension and about 2.5 m height to damp any air movement during the test period. Four vertical sides covered partially with a thick nylon synthetic fabric leaving uncovered 200 mm above the ground level to allow free air movement through from the bottom and top sides of the shield and around the apparatus during the test period. To facilitate entering to the test rig during the orientation setting time, access opening through the shield has been made while all the setting adjustment and measurement devices have been arranged outside and adjacent to the nylon shield. Radiation heat losses from the aluminum cylinder is partially between cylinders in the array and with the surrounding. Despite the dissimilarity of the radiation thermal exchange for each individual cylinder in the array, the exchange of thermal radiation between the cylinders very small and can be neglected as the emissivity of polished aluminum surface in the worst case is low (approximately 0.25 [13]) and due to the uniformity and low temperature difference between cylinders of the array. The heat loss by radiation was evaluated experimentally depending upon shape factor equation tabulated in the textbook and was found to be varying between 2.6% - 4.3% of the total input power.

### Experimental Procedure

Daily preparation and checking for the apparatus is required including the whole apparatus level, the five cylinders thermocouples and electrical circuits and the spacing and configuration of the cylinder. The array inclination angle then adjusted as required and the stabilized electric power supply was switched-on then the wattmeter

readings adjusted to give the identical power for all array cylinders. All thermocouples readings were recorded every half an hour using digital electronic thermometer until the condition of steady-state achieved. To reach steady-state condition for the first run, approximately 4 hours is required and the steady-state obtained when the thermocouples temperatures reading remain unchanged or vary no more than 0.5 ° C within last 30 minutes. The final temperature readings then recorded for this test run and also for this run the ambient temperature, the watt meters reading and the Teflon end pieces thermocouples reading. The steady-state condition was found will be shorter (within 2 hours) as the heater's power is kept constant while the array orientation change only.

### Data Reduction

The cylinders arrangement in staggered array configuration is depicted in Fig.(3). The cylinders traversing separation distance  $S_T$  is equal to 2.5D while the cylinders a longitudinal separating distance  $S_L$  is equal to 5D. This array arrangement gives the longitudinal surface to surface separating distance  $b_L$  equal to 4 D while the diagonal surface to surface separating distance  $b_d$  equal to 2.5355 D calculated using the following formula:

$$b_d = \left( (S_T)^2 + \left( \frac{S_L}{2} \right)^2 \right)^{\frac{1}{2}} - D \quad (1)$$

To analyze the natural convection heat transfer process, simplified steps were followed depending upon the experimental data collected from the experimental apparatus. The total input power supplied  $Q_{tot}$  to each individual cylinder depends upon the wattmeter reading. The power supplied is converted to heat in the individual cylinder in the array. For steady-state conditions and the energy balance, all the heat supply and heat losses and the convective heat loss can be written as follows:

$$Q_{conv} = Q_{tot} - Q_{cond} - Q_{rad} \quad (2)$$

$Q_{cond}$  is the total Teflon pieces conduction heat losses and evaluated from:[14]:

$$Q_{cond} = k_{Teflon} \cdot A_{Teflon} \cdot \left( \frac{dT}{dx} \right) \quad (3)$$

Where  $A_{Teflon}$  represents the annular cross-sectional area of the Teflon piece  $k_{Teflon}$  represents the thermal conductivity of the Teflon and  $\frac{dT}{dx}$  is the axial temperature gradient in the Teflon piece evaluated by the temperature the difference for the 10 mm apart measured by two thermocouples impeded in the Teflon piece. The  $Q_{cond}$  calculated for both ends of each heated cylinder in the array. The conduction ends loss may be similar for the horizontal array case but it becomes dissimilar for inclined and vertical cases.

The following formula can be used to calculate radiation heat loses:

$$Q_{rad} = A_s \cdot \varepsilon \cdot \sigma \cdot F \left( T_{av-1}^4 - T_{av-2,a}^4 \right) \quad (4)$$

For two long parallel cylinders, the shape factor is given by [14]:

$$F_{1-2} = F_{2-1} = \frac{1}{n} \left( (X^2 - 1)^2 + \sin^{-1} \left( \frac{1}{X} \right) - X \right) \quad (5)$$

$$\text{Where } X = 1 - \left( \frac{S_T}{D} \right) \quad (6)$$

Where  $\sigma$ : Stephan-Boltzmann constant =  $5.669 \cdot 10^{-8} \text{ W/K}^4 \cdot \text{m}^2$ .

Where are the cylinders center to center spacing and  $D$  is the cylinder diameter. The shape factor between the considered cylinder and the ambient,  $F_{1-a}$  evaluated by:

$$F_{1-a} = 1 - F_{1-2} \quad (7)$$

The value between 0.85 and 0.95 gives an appropriate value of  $F_{1-a}$  [13]. The heat exchange by radiation between the specific cylinder and the other cylinders or with the ambient calculated separately and as  $T_{av-1}$  represent the specific cylinder average surface temperature and  $T_{av-2,a}$  represent either other cylinder average surface temperature or ambient temperature. Also the shape factor either  $F_{1-a}$  or  $F_{1-2}$ . The convective heat flux can be calculated

$$q_{\text{conv}} = \left( \frac{Q_{\text{cond}}}{A_s} \right) \quad (8)$$

$$\text{Where: } A_s = \pi \cdot D \cdot L \quad (9)$$

On this convective heat flux the local and average heat transfer coefficient and all the local and average Nusselt number calculated as follow. First the local heat transfer coefficient evaluate from:

$$h_x = \frac{q_{\text{conv}}}{(T_{s,x} - T_a)} \quad (10)$$

Where  $T_{s,x}$  represent the local surface temperature. The local Nusselt number  $Nu_x$  depends on the local heat transfer coefficient and surface axial distance and evaluated from.

$$Nu_x = \frac{h_x \cdot x}{k_x} \quad (11)$$

While the local Nusselt number  $Nu_{x,D}$  based on the cylinder diameter calculate as:

$$Nu_{x,D} = \frac{h_x \cdot D}{k_x} \quad (12)$$

The air thermal conductivity  $k$  and all the air physical properties come after evaluated at the mean film temperature as reported in [15]:

$$T_{f,x} = \frac{(T_{s,x} + T_a)}{2} \quad (13)$$

The local Grashof number based on cylinder axial distance  $x$  evaluated as:

$$Gr_x = \frac{g \cdot \beta \cdot (T_{s,x} - T_a) x^3}{\nu_x^2} \quad (14)$$

The local Grashof number based on cylinder diameter  $D$  evaluated as:

$$Gr_{x,D} = \frac{g \cdot \beta \cdot (T_{s,x} - T_a) D^3}{\nu_x^2} \quad (15)$$

The average heat transfer coefficient calculated for different cylinder length  $L$  as follows:

$$h_L = \frac{1}{L} \int_{x=0}^{x=L} h_x dx \quad (16)$$

The average Nusselt and Grashof numbers for different cylinder length can be calculated from:



$$Nu_L = \frac{h_L \cdot L}{k_L} \quad (17)$$

$$Gr_L = \frac{g \cdot \beta \cdot (T_{s,L} - T_a) \cdot L^3}{\nu_L^2} \quad (18)$$

The average Nusselt and Grashof numbers based on the cylinder diameter D can be calculated from:

$$Nu_{L,D} = \frac{h_L \cdot D}{k_L} \quad (19)$$

$$Gr_{L,D} = \frac{g \cdot \beta \cdot (T_{s,L} - T_a) \cdot D^3}{\nu_L^2} \quad (20)$$

The average surface temperature  $T_{s,L}$  for different cylinder length L can be calculated from:

$$T_{s,L} = \frac{1}{L} \int_{x=0}^{x=L} T_{s,x} dx \quad (21)$$

All the air physical properties to evaluate  $Nu_{av}$  and  $Gr_{av}$  numbers were evaluated at the mean film temperature Burmeister, [15]

### Experimental Error Analysis

The uncertainty of experimental results have been analyzed for experimental variables measured following the Method explained and reported in Holman [16] which depends on each individual variable percentage error accounted in experimental measurement devices and also depends upon the effect of this measured variables on the physical properties. Such variables are air and surface temperatures, air properties, linear measurement of cylinders diameters and lengths and electrical heater input power which were found  $\pm 0.5\%$ ,  $\pm 0.18\%$ ,

$\pm 0.73\%$  and  $\pm 0.45\%$ , respectively. The combined effect of these variables measured percentage error on the measured dimensionless groups such as Reynolds number, Nusselt number, and Prandtl number were 3.8%, 2.74%, and 2.5 %, respectively.

## RESULTS AND DISCUSSIONS

In the present staggering cylinder arrangement, the system comprises five cylinders symbolized for demonstration as P0 - P<sub>4</sub> and depicted in fig.(3) . Cylinders P<sub>0</sub>, and P<sub>3</sub> located at the array left and right lower corners, cylinder P<sub>1</sub> is located at the array center and cylinders P<sub>4</sub> and P<sub>2</sub> located the array left and right upper corners when the array-oriented horizontally. The arrangement establishes, for the horizontal array, the cylinders P<sub>4</sub> and P<sub>2</sub> are directly above the P<sub>0</sub> and P<sub>3</sub> respectively. The array tested has the configuration of longitudinal ( in the flow direction) and traversing distances of 2.5 D and 5D, respectively. Each individual cylinder in the array cylinder has a length of 500 mm, outside diameter of 25.4 mm and a wall thickness of 2 mm. A total of 20 test runs were executed on this configuration for five array orientation angles 0° , 30 °, 45 °, 60 ° and 90 ° ( vertical ) and for each of these array orientation ,cylinders in the array was subjected a four constant wall heat fluxes varied from 621.58 W/m<sup>2</sup> to 1350 W/m<sup>2</sup>).

### Variation of Surface Temperature along the Cylinder Length

The local surface temperature  $T_x$  variation along the cylinder axial position x, for five array inclination angles 0° , 30 °, 45 °, 60 ° and 90 ° presented for maximum heat flux (1350 W/m<sup>2</sup>) is presented for three cylinders P<sub>0</sub>, P<sub>1</sub> and P<sub>4</sub> in

Figs.(4),(5) and (6), respectively. The general temperatures distribution shape shows that it approximately for the same orientation, repeated itself as the cylinder heat flux changes while changing cylinder orientation also affect the temperature distribution general shape. The general shape, with an exception for the horizontal array, shows a rapid increase in surface temperature at the lower part of the cylinder in the array to reach maximum value than the shape approximately remains constant and then temperature drop at the cylinder uppermost part. This shape indicates that the whole of the cylinder length is covered with the laminar flow at the lower part of the cylinder and the end conduction heat transfer affect the distribution and makes it drop at the cylinder uppermost part. The temperature distribution for the horizontal array shows, for specific surface heat flux, constant temperature for the whole cylinder length with a small temperature drop at both cylinders ends and that attributed to the cylinder conduction end losses. As the power supply is constant with time and identical for all array five cylinders, a similarity temperature distribution obtained the left and right sides of the array and for all array orientations. That indicates that the temperature distribution results of cylinder  $P_3, P_1$  and  $P_0$  are similar while cylinder  $P_2$  is similar to  $P_4$ . Therefore, the analysis focused on the left side of the array which covered three cylinders  $P_0$  (left lower corner),  $P_1$  (central cylinder) and  $P_4$  (left upper corner) in the horizontal array situation. The results depicted in Fig. (4) and Fig. (5), for cylinder  $P_0$  and  $P_1$  reveals a similar distribution for all range of heat flux and orientation applicable in the present investigation. Results reveal that the cylinders traversing spacing  $S_T$  and longitudinal spacing  $S_L$  deployed is sufficient to prevent the first cylinder  $P_0$  natural convection flow to interfere with convection flow field of the first cylinder of the adjacent column  $P_1$  Fig.(6) shows the effect of natural convection flow of first row cylinders ( $P_0$  and  $P_3$ ) on the second row cylinders ( $P_4$  and  $P_2$ ) in the array which is very clear for horizontal and inclined array and this effect diminished for the vertical array,

#### Variation of Local Heat Transfer Coefficient along the Cylinder Length

The local heat transfer coefficient  $h_x$  variation along the cylinders length  $x$  for different array inclination is demonstrated, for three cylinders  $P_0$ ,  $P_1$ , and  $P_4$  (left side of the array), in Fig. (7), Fig. (8) and Fig (9) respectively. These figures were depicted for the same runs shown in figures (4-6) which is subjected to heat flux equal to  $1350 \text{ W/m}^2$ . The general local heat transfer coefficient  $h_x$  distribution shape shows that it approximately for the same orientation, repeated itself as the cylinder heat flux changes while changing cylinder orientation also affect the temperature distribution general shape. The general shape, with an exception for the horizontal array, shows a rapid decrease The local heat transfer coefficient  $h_x$  at the lower part of the cylinder in the array to reach minimum value than the shape approximately remains constant and then coefficient  $h_x$  value slightly improved at the cylinder uppermost part. At the cylinder leading edge ( $x = 0$ ) and for the vertical and inclined array, distribution reveals a high value of  $h_x$  as the result of expecting zero boundary thickness at cylinder leading edge then  $h_x$  value decreases rapidly to reaches minimum value at a specific  $x$  location. This reduction in  $h_x$  value is due to thermal boundary layer development. The improvement of  $h_x$  at cylinder uppermost can be attributed partly to the boundary layer transition from laminar mode to turbulent mode and another part due to axial condition heat loss via the Teflon piece. The flow separation can be expected, For the inclined array while the flow climbs upward along array cylinders and separation will complicate the prediction and boundary layer behavior. The flow separation trends expected to dominate the heat transfer process in the array inclination range between  $30^\circ$  to  $60^\circ$ . The reduction of cylinder inclination angle natural convection flow to be climb along the cylinder circumference for horizontal cylinder and that makes the local heat transfer coefficient does not vary with cylinder length. Results for different heat flux also reveals that the  $h_x$  values at the same value of  $x$  increase, as it should, with the increases of heat flux.

### Variation of Average Heat Transfer Coefficient along the Cylinder Length

The average heat transfer coefficient  $h_L$  variation along the array cylinders length  $L$ , for cylinders  $P_0$ ,  $P_1$  (central) and  $P_4$  is depicted in Figures (10), (11) and (12), respectively. These figures show for three cylinders at same heat flux ( $q = 1350 \text{ W/m}^2$ ) but they have been oriented from  $\theta$  equal to  $0^\circ$  (horizontal) to  $\theta$  equal to  $90^\circ$  (vertical). In general, the  $h_L$  values for cylinder  $P_3$  is similar to cylinder  $P_0$  while  $h_L$  for cylinder  $P_2$  is similar to cylinder  $P_4$ . The horizontal cases show  $h_L$  values increase with increasing of surface heat flux for the array separating distance ( $S_L$  and  $S_T$ ) tested. The results for the inclined array, which are shown in the same figures, illustrate a high  $h_L$  value at cylinder leading edge ( $L=0$ ) and the value decreases gradually to a minimum value at tube uppermost part. For the vertical array, the results show, for all cylinders in the array,  $h_L$  value similar to the inclined cylinder with  $h_L$  values become constant and goes asymptotically with to the x-axis with a very limited improvement at the uppermost part of the cylinder and this can be attributed to the heat transfer process transition from laminar to transition or maybe turbulent at the cylinder upper most part.. Obviously, as  $L$  approach zero,  $h_L$  must approach infinity as zero boundary layer thickness at the cylinder leading edge. For inclined and vertical array, the general shape for  $h_L$ , shifted upward as the heat flux increases for the same orientation. The last  $h_L$  values for the five cylinders in the array and for 20 runs tested for four heat flux varies between  $630 \text{ W/m}^2$  to  $1350 \text{ W/m}^2$  have been used in the further experimental heat transfer data analysis leading to data correlation as those values represents for the complete cylinder length.

### Correlation of Average Heat Transfer Results

The average Nusselt number ( $Nu_{L,D}$ ) based on the whole cylinder heat transfer coefficient  $h_L$  variation with ( $Gr_{L,D}$  Pr) is demonstrated for three cylinders ( $P_0$ ,  $P_1$ , and  $P_3$ ) in Fig. (13) and for cylinders  $P_4$  and  $P_2$  in Fig. (14), for all heat flux ranges, and for all angles of inclinations. The presentation is based on the results shown before as the three cylinders  $P_0$ , and  $P_3$  (lower corners in bundles) and  $P_1$  (bundle central) have got identical results for all inclination angles and the present cylinder spacing does not show any flow interference between the lower corners cylinders and the central cylinder. Therefore, the three cylinders behave as a single cylinder. The variations of average Nusselt number depicted in Fig.(14) for  $P_2$  and  $P_4$  in the array, show a clear enhancement in the heat transfer process in comparison with a single cylinder heat transfer process for the configuration of the present cylinders in the array. That can be assigned to the lower cylinders plume which has been cited in some previous literature. The ascending plume maybe enhanced or decline the heat transfer process depending upon cylinder configuration and spacing criteria. The heat transfer enhancement occurs as the plume changes the convective regime from a pure natural convection regime to a mixed free and forced convection regime. As the natural convection heat transfer process is highly dependent on the hot surface geometry, several correlations exist to evaluate the heat transfer coefficient The experimental data analysis should be based on a reference characteristic length weather based on the cylinder diameter  $D$  as the characteristic length ( horizontal cylinder natural flow around cylinder circumference) or cylinder length  $L$  (vertical cylinder natural flow along cylinder axis) or employs either ( $L/D$ ) or angle  $\theta$  as a characteristic parameter. The average heat transfer results presented for whole cylinder length  $L$  and depicted in Fig.(13) and (14) employed the heat transfer dimensionless groups based on cylinder diameter  $D$ . The figures were presented as  $\log(Nu_{L,D})$  against  $\log(Gr_{L,D} Pr)$  and a group straight lines each represent one of the array orientation. For the present investigation, diameter and length of the cylinder and experiments heat flux tested make declare our results completely in the laminar region and all references mention before indicated that the dimensionless group governed by a power function rose to 0.25 in this region. The results, demonstrated in the Fig.(13) and (14) on a log-log the power

function in groups having of straight lines with a slop nearly equal to 0.25. The general equations of these straight lines are in the form of equation (22).

$$\text{Log}_{10}(\text{Nu}_{L,D}) = \text{Log}_{10}(C') + m \text{Log}_{10}(\text{Gr}_{L,D} \cdot \text{Pr}) \quad (22)$$

$$\text{Where } C = 10^{\text{log}_{10}(C')} \quad (23)$$

Equations also show that array orientation has a very limited effect on slop (m) value of the correlation equations (22). The experimental data analysis deviate within  $\pm 4\%$  of the correlation lines. Correlation equations have been tabulated in the table (1) for different array orientation  $\theta$  which evaluated for five cylinders and cylinders configuration in the array mentioned before. For the array cylinders, the effect of array orientation is evident in equations C values. For the case of a vertical array, results reveal that all cylinders have the same heat transfer results with the configuration presented and the vertical array has the lowest heat transfer in comparison with other array orientations. Therefore, the results of vertical cylinders are used for comparison and to demonstrate the enhancement in the heat transfer process for different array orientation. These enhancement values as a percentage and the C values are tabulated in the table (2). Using the same experimental data analysis procedure to evaluate the average heat transfer for the whole length of the cylinder and for all orientation based on D reveals that the enhancement in heat transfer process increases to approximately 17% takes place as the single-cylinder merely moves from vertical to horizontal. To expose such enhancement in heat transfer and to demonstrate array orientation graphically, Fig.(15) depicted to show the variation of the dimensionless parameter  $(\text{Nu}_{L,D} / (\text{Gr}_{L,D} \cdot \text{Pr})^{0.25})$  with array inclination angle  $\theta$ .

### Comparison with Previous Works

For a single horizontal tube (tube  $P_0$  results), the average heat transfer coefficient was calculated and  $P_0$  correlation results allow for providing the estimation and comparison basic of the heat transfer rate of other tubes in the horizontal array. The calculated values are correlated for the laminar natural convection range by the following formula:

$$\text{Nu}_{av} = 0.4802 (\text{Ra})^{0.25} \quad (24)$$

For a single horizontal cylinder, The above equation affords an average Nusselt number rather in a good agreement with correlation proposed by Morgan [1] and equation (24) contributes an average Nusselt number higher than those [1] by (0.0416%). For array cylinders in a vertical orientation, the results are approximately governed by a unique equation with C value equal to 0.408 which is in contradiction and disagreement with some of the previous work result of Tokura et.al [7] can be utilized to show the cylinders heat transfer interactive effect within an array. Results, for each specific arrangement (b/D), are manifested in the form of average Nusselt ratio  $(\text{Nu}_i/\text{Nu}_s)$  variation, where i acts as the cylinder number in the array while s acts as the results for a single-cylinder (the bottom cylinder in the array), and with the parameter  $(S_i/S_{\max})$ , where  $S_i$  acts as individual cylinder center to center separating distance measured from the bottom cylinder while  $S_{\max}$  acts as the maximum center to center cylinder separating distance between the bottom and top cylinders in the array. Results disclose that a reduction in  $(\text{Nu}_i/\text{Nu}_s)$  value as  $(S/S_{\max})$  increases for (b/D) less than (1), then remain constant for (b/D) equal to(1) and increases as for (b/D) greater than(2), for the same Ra number. This result also is in a good agreement with the present result with (b/D) equal 5 for cylinders  $P_2$  and  $P_4$  which give a higher result than that obtained for the of three cylinders in the bottom of the array  $P_0$ ,  $P_3$ , and  $P_1$ .

## CONCLUSIONS

Natural convection heat transfer to air from an inclined five cylinders array set up in staggered shape and subjected all to constant heat flux, investigated experimentally. The staggered array with fixed transversing  $S_T$  and longitudinal  $S_L$  spacing equal to 2.5 D and 5 D, respectively. The array orientations are 0°, 30°, 45°, 60° and 90° (vertical). From the experimental results the following conclusions can be achieved:-

- The surface temperature variation for the inclined and vertical array has the same general shape which increases at the cylinder lower part with a reduced rate at upper part as the boundary layer build-up to reach a constant then drop the temperature at the cylinder most upper part. An approximately constant temperature distribution depicts along the cylinder length for the horizontal array. These distributions change and demonstrate increases and decreases with increasing and decreasing the applied cylinder surface heat flux. For approximately the same heat flux and laboratory air temperature, the distributions show a surface temperature reduction as the array orientation change from vertical to horizontal. The temperature distributions, for a horizontal and inclined array and for cylinders  $P_2$  and  $P_4$ , have got a lower surface temperature than cylinders  $P_1$ ,  $P_0$ , and  $P_3$  for same array orientation and same heat flux. The horizontal array has on average lowest surface temperature and best heat transfer dissipation. The temperature distribution also exposes that for the configuration of the tested cylinders the natural convection flow for central cylinder doesn't interfere with another cylinder in the array for all array orientation.
- Local and average heat transfer coefficients ( $h_x$  and  $h_L$ ) variations along the array cylinders for inclined and vertical array show a sharp reduction at the lower part of the cylinder then to be a constant or little improving at cylinder uppermost part of the cylinder and that attribute to the laminar boundary layer domination the flow and heat transfer process along the array cylinders. For the same angle of inclination, Local and average heat transfer coefficients increase with the increasing surface heat flux and for an individual cylinder in the array and for same heat flux, the local and average heat transfer coefficients decrease as the cylinder orientation change from horizontal to vertical. For horizontal and inclined array and for the same heat flux, heat transfer coefficients for cylinders  $P_2$  and  $P_4$  show a clear enhancement in heat transfer process in comparison with cylinders  $P_0$ ,  $P_1$ , and  $P_3$  while the central cylinder coefficients exhibit no effect in the present configuration.
- Relations between cylinder average Nusselt number  $Nu_{L,D}$  and the cylinder  $Gr_{L,D} Pr$ , for the experimental data, were correlated. The correlation demonstrated that the array orientation has no effect on the correlation slope (m) as it stays having approximately 0.25 which can be attributed to domination of the laminar natural convection heat transfer for all the cases have been investigated. The correlation expressed a clear effect of the array orientation on the correlation C value. For all array orientation correlation equations for all cylinders and have been tabulated. Heat transfer enhancements as percentages and the C values all cylinders in the array also tabulated. The enhancement in the heat transfer process for an inclined and horizontal bundle can be attributed to the change in heat transfer from laminar natural convection to mixed convection under the effect of lower cylinder natural convection convective flow which interferes with upper cylinder boundary layer.
- A comparison with available previous work which studied vertical and horizontal single-cylinder shows that the heat transfer results in an acceptable agreement with the horizontal single-cylinder but in contradictory results with a vertical cylinder.

## ACKNOWLEDGMENT

This work has been performed at the Nuclear Engineering Department, College of Engineering University of Baghdad, Iraq. The authors would truly like to recognize college of engineering for providing technical financial assistance without it this work is difficult to complete successfully.

## REFERENCES

1. **Morgan, V.T.**, (1975) "The Overall Convection Heat Transfer from Circular Cylinders", in *Advances in Heat Transfer*, Vol.11. Academic Press New York, pp 199–264.
2. **Oothuizen, P.H.**, (1976) "Experimented Study of Free Convection From Inclined cylinder", *Journal of Heat Mass Transfer*, pp 672–674 ,November
4. **Al-Arbi M. and Salman, Y. K.** 'Laminar Natural Convection Heat Transfer from an Inclined Cylinder.' *Int. J. Heat Mass Transfer*, Vol. 23, PP (45–51). 1980.
5. **Popiel, C. O., Wojtkowiak, J., and Bober, K.** (2007), 'Laminar free convective heat transfer from isothermal vertical slender cylinder', *Experimental Thermal and Fluid Science*, 32 , pp. 607–613.
6. **Marsters, G.F.**, (1972) "Arrays of Heated Horizontal Cylinders in natural Convection" *Int. Journal of Heat and Mass Transfer*, 15 (5), pp. 921–933.
7. **Sparrow, E.M. and Niethammer, J.E.**, (1981) "Effect of Vertical Separation Distance and Cylinder –to–Cylinder Temperature Imbalance on Natural Convection for a Pair of Horizontal Cylinder "ASME, *Journal of Heat Transfer*, Vol. 103(4),pp. 638–644 .
8. **Tokura, H. Saito, Kiohinami, K. and Muramoto, K.**, (1983) "An Experimental Study of Free Convection Heat Transfer From a Horizontal cylinder in a vertical Array Set in Free Space between Parallel Walls" ,*Journal of Heat Transfer*, Vol. 104 , pp. 102–107.
9. **Karvinen, R. and Kauramaki, T.**, (1986) "Effect of Orientation on Natural Convection of a Cylinder Array in Water". *INT. Comm. Heat Mass transfer*, Vol.13, pp.155–161.
10. **Reymond, O., Murray, D. B., and O'Donovan ,T. S.** (2008) , ' Natural convection heat transfer from two horizontal cylinders ', *Experimental Thermal and Fluid Science* 32 , pp. 1702–1709.
11. **Chouikha,\*R., Guizania, A., El Cafsib, A., Maaleja, M. And Belghith, A.** (2000). ' Experimental study of the natural convection flow around an arrayof heated horizontal cylinders'. *Renewable Energy* 21 PP 65–78.
12. **Chouikh R, Guizania A, Maañ lej M, and Belghith A.** (1999), 'Numerical study of the natural Convection flow around an array of two horizontal isothermal cylinders',. *Int. Com Heat Mass Transfer*; 13(1):77–88.
13. [12]. **Sparrow, E.M and Boessneck, DS.** (1983),; *Effects of transverse misalignment on natural Convection from a pair of horizontal cylinders', J. Heat Transfer* 105, 241–247 (1083)(Journal Article)
14. **Lienhard IV, J.H. And Lienhard V, J.H.**(2004) 'A Heat Transfer Text Book', Third Edition, Published by Phlofiston Press Cambridge Massachusetts USA.

15. *Bejan, A, (1995), 'Convection Heat Transfer'. Second Edition. John Wiley & Sons Inc.: New York.*
16. *Burmeister, Louis C (1993), 'Convective Heat Transfer'. John Wiley & Sons, Inc.: New York.*
17. *Holman, J.P. (2001) 'Experimental Methods for Engineers, seventh ed., Mc-Graw Hill International Edition, New York, USA, 2001.*

**APPENDICES**

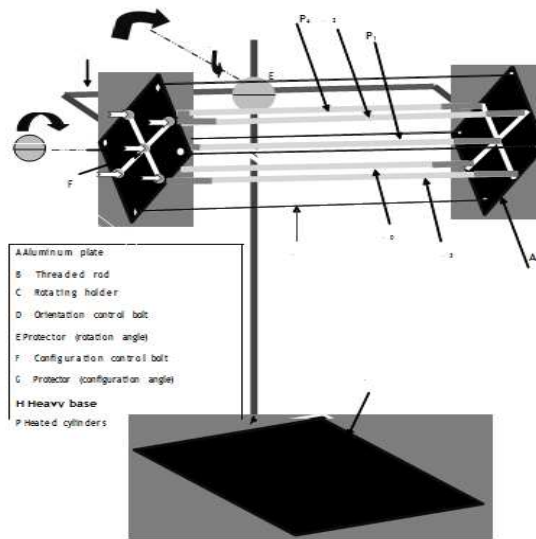


**Figure 1**

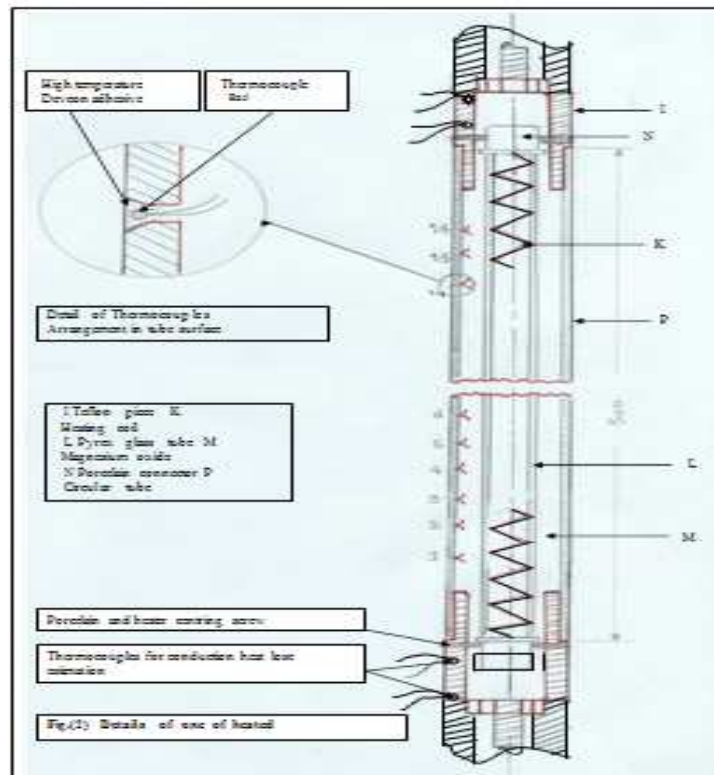


**Figure.2: General Arrangement of the Apparatus**

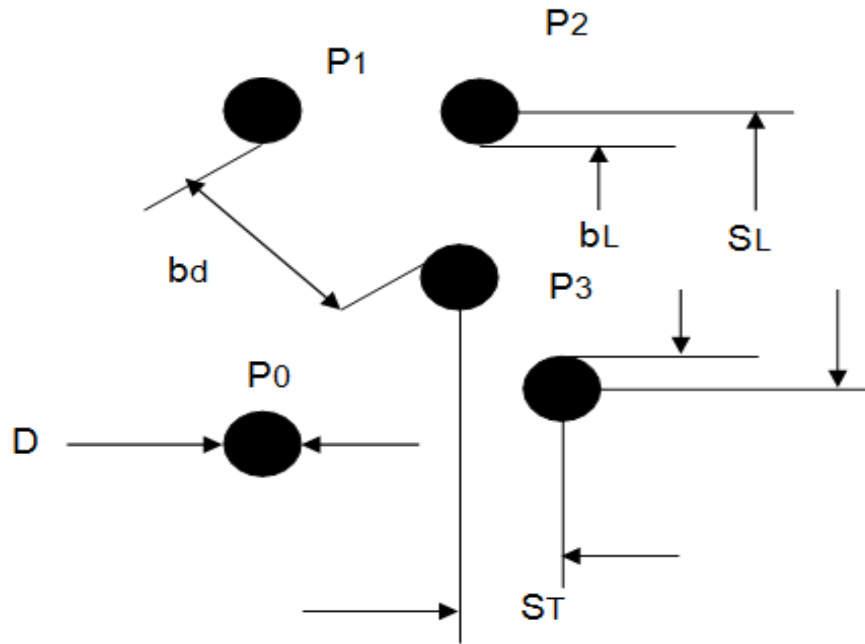


Figure 3: Cylinders Arrangement in the Staggered Bundle

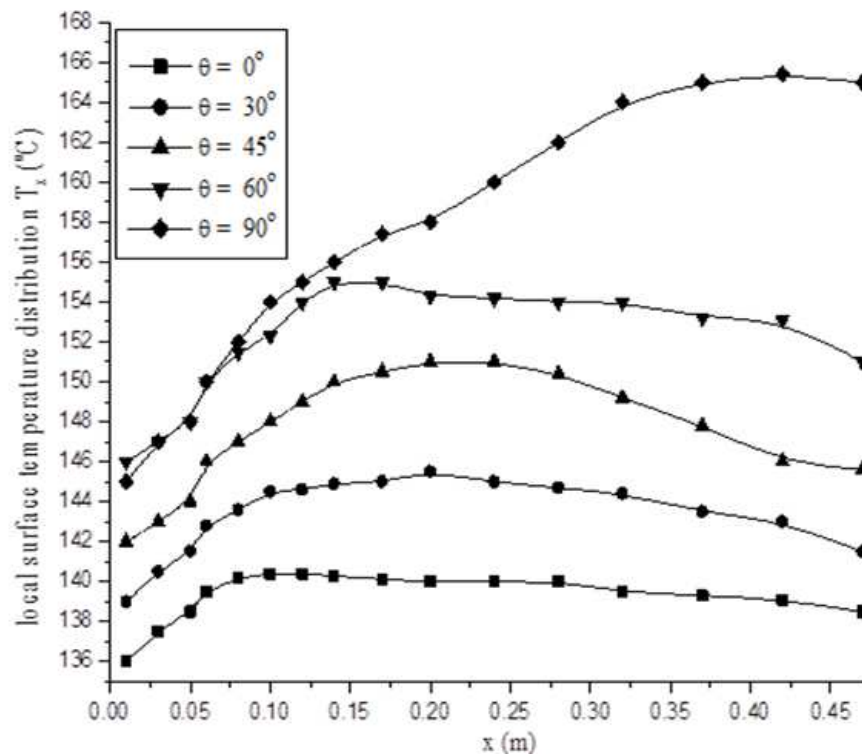


Figure 4: Variation of Local Surface Temperature Distribution  $T_x$  along Cylinder  $P_0$  for Different Staggered Bundle Orientations,  $Q = 1350 \text{ W/M}^2$



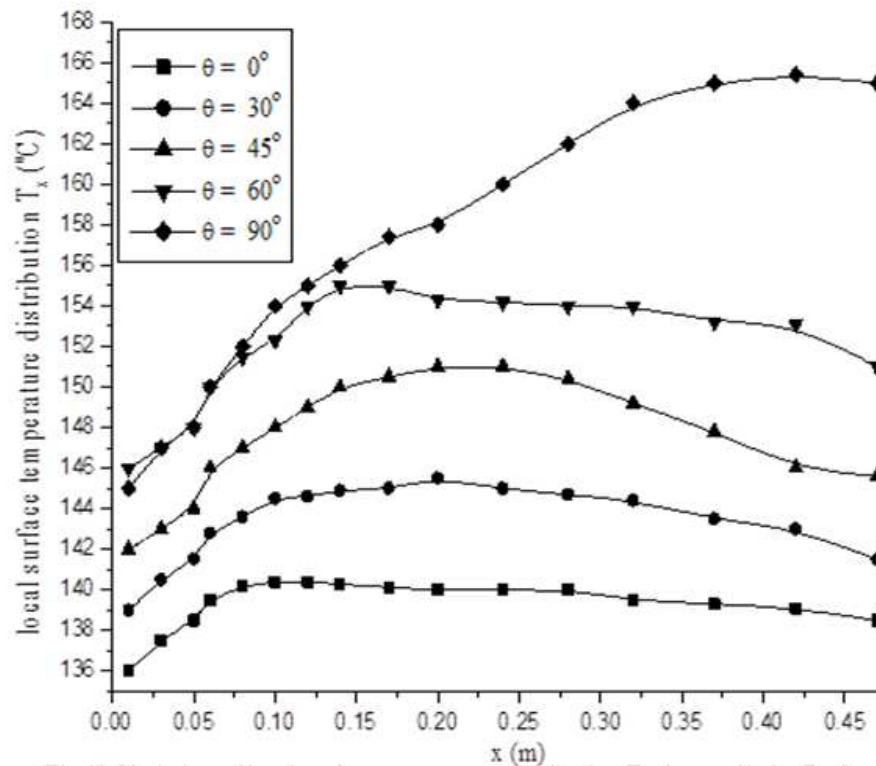


Figure 5: Variation of Local Surface Temperature Distribution  $T_x$  Along Cylinder  $P_1$  for Different Staggered Bundle Orientations,  $q = 1350 \text{ W/m}^2$

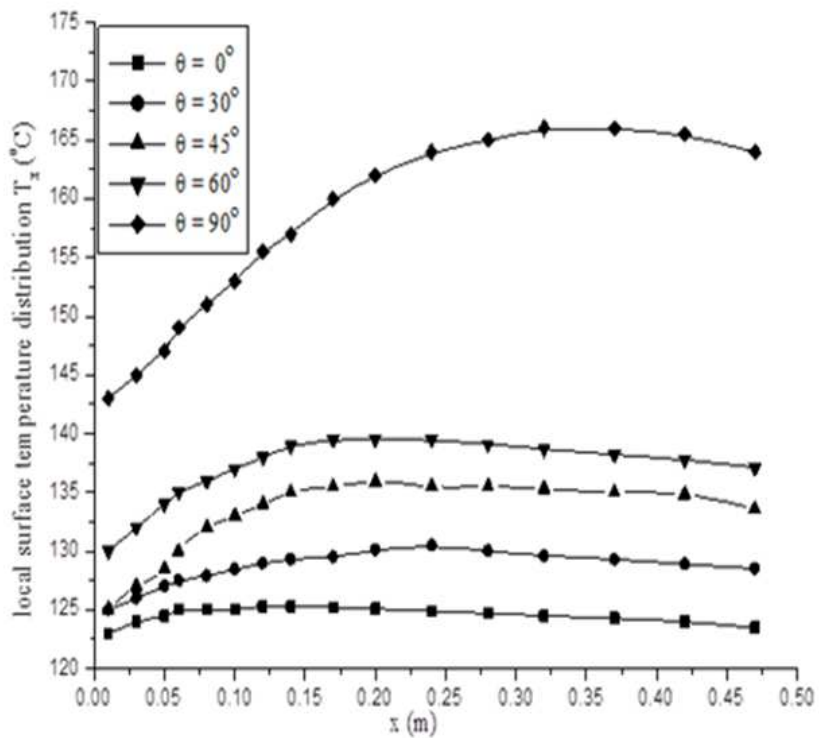


Figure 6: Variation of Local Surface Temperature Distribution  $T_x$  Along Cylinder  $P_4$  for Different Staggered Bundle Orientations,  $q = 1350 \text{ W/m}^2$

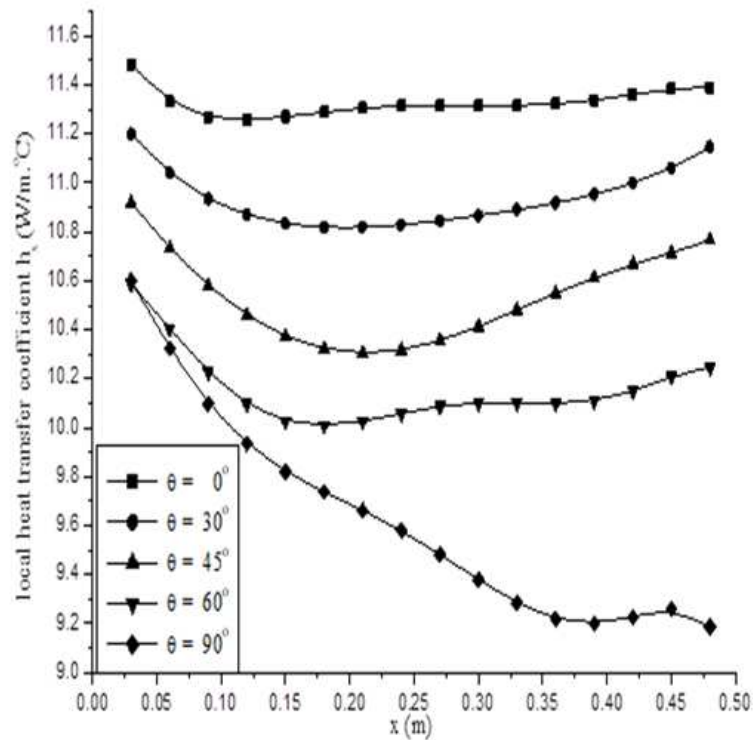


Figure 7: Variation of Local Heat Transfer Coefficient  $h_x$  Along Cylinder  $P_2$  for Different Staggered Bundle Orientations,  $q = 1350 \text{ W/m}^2$

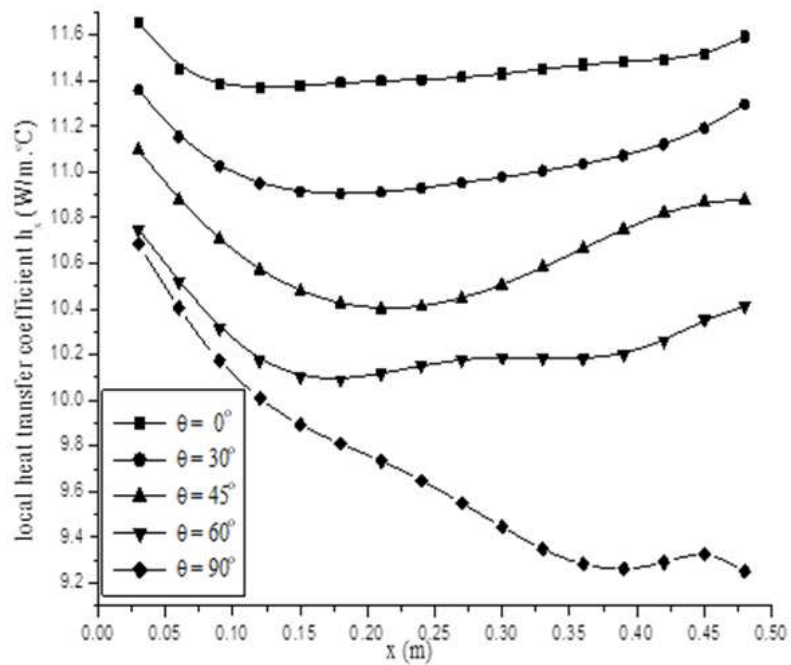


Figure 8: Variation of Local Heat Transfer Coefficient  $h_x$  along Cylinder  $P_1$  for Different Staggered Bundle Orientations,  $q = 1350 \text{ W/m}^2$

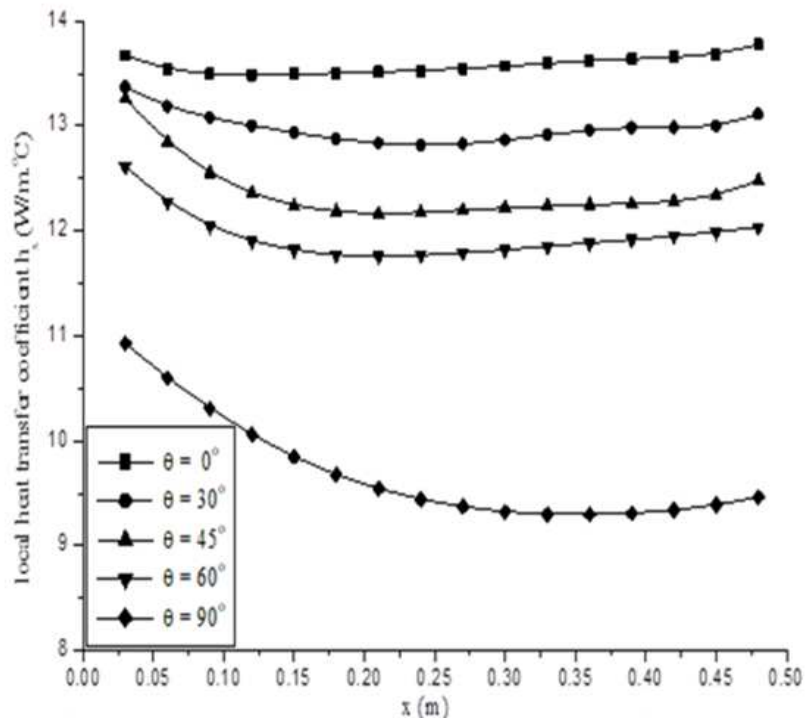


Figure 9: Variation of Local Heat Transfer Coefficient  $h_x$  Along Cylinder  $P_4^2$  for Different Staggered Bundle Orientations,  $q = 1350 \text{ W/m}^2$

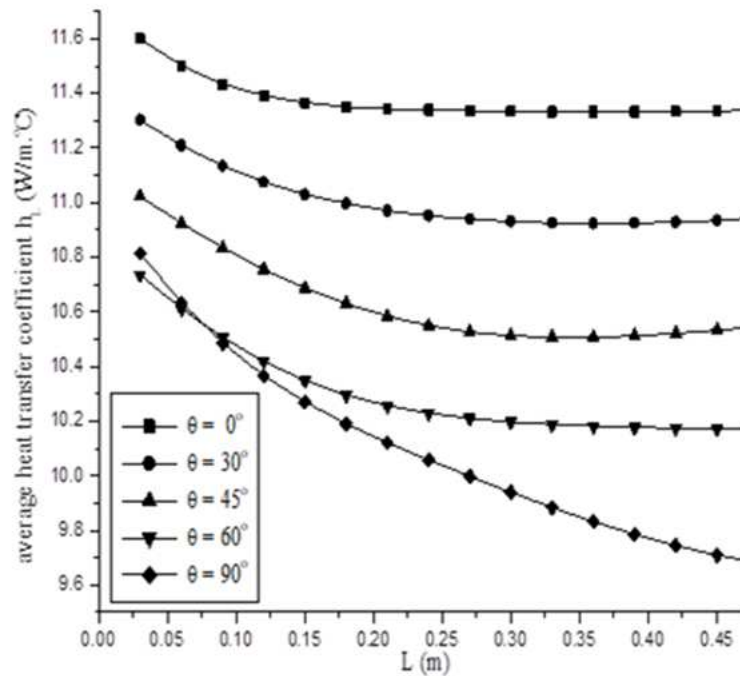


Figure 10: Variation of Average Heat Transfer Coefficient  $h_1$  Along Cylinder  $P_6^2$  for Different Staggered Bundle Orientations,  $q = 1350 \text{ W/m}^2$

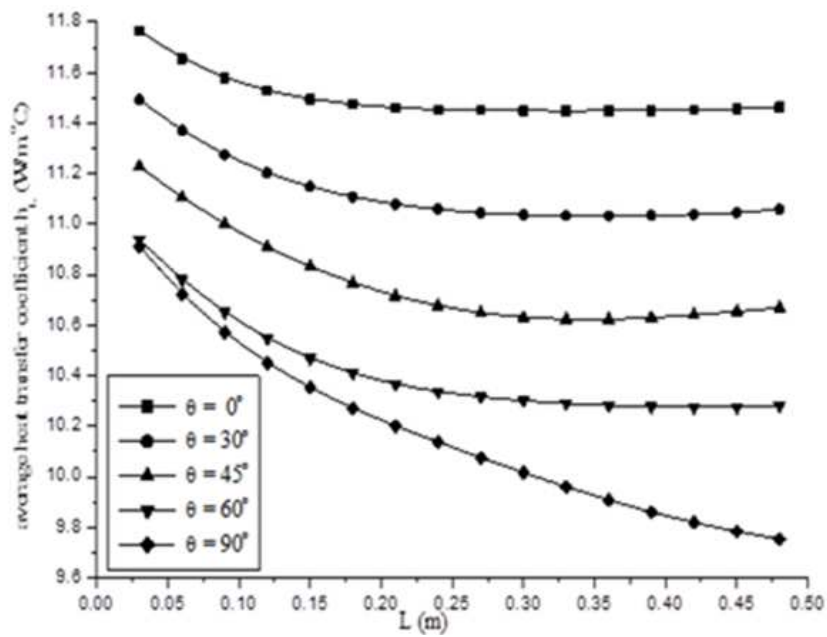


Figure 11: Variation of Average Heat Transfer Coefficient  $h_2$  along Cylinder  $P_1'$  for different Staggered Bundle Orientations,  $q = 1350 \text{ W/m}^2$

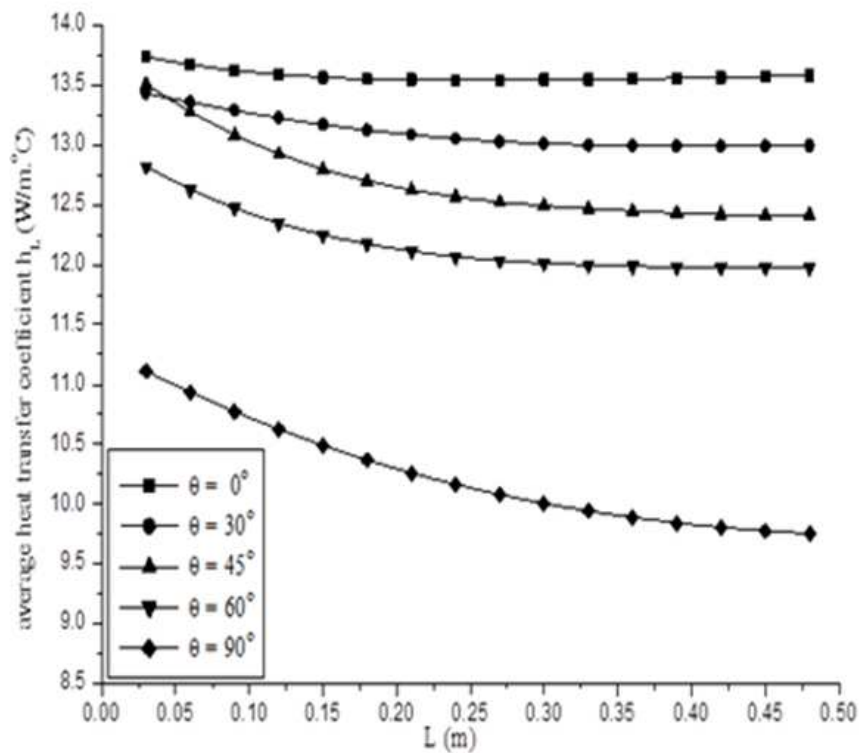


Figure 12: Variation of Average Heat Transfer Coefficient  $h_2$  Along Cylinder  $P_1'$  for Different Staggered Bundle Orientations,  $q = 1350 \text{ W/m}^2$

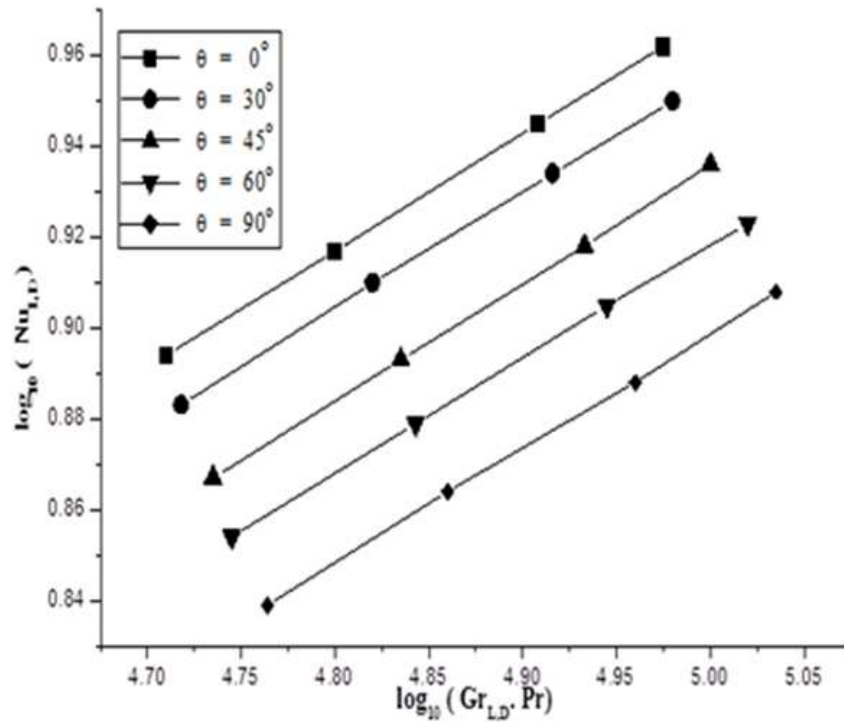


Figure 13: Variation of  $\text{Log}_{10} Nu_{LD}$  with  $\text{Log}_{10} (Gr_{LD} Pr)$  for Different Staggered Bundle Orientations and Cylinders  $P_0$   $P_3$  and  $P_1$

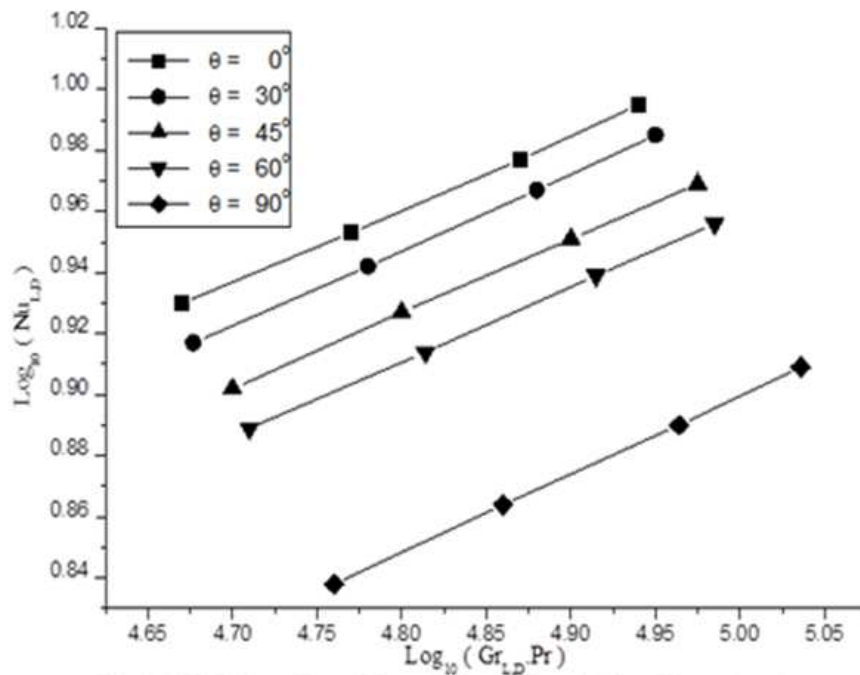


Figure 14: Variation of  $\text{Log}_{10} Nu_{LD}$  with  $\text{Log}_{10} (Re_{LD} Pr)$  for Different Staggered Bundle Orientations and Cylinders  $P_4$  and  $P_2$

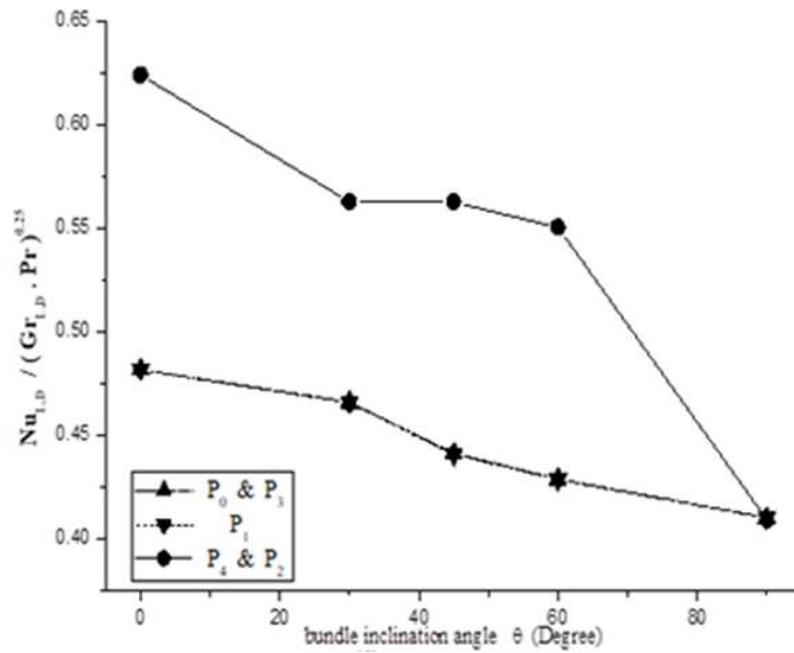


Figure 15: Variation of  $Nu_{L,D}/(Gr_{L,D} Pr)^{0.25}$  for with Bundle Inclination Angle  $\Theta$  for Staggered Bundle having Cylinders Separation Distances  $S_1$  &  $S_2$  Equal to  $5d$  &  $2.5d$ , respectively

Table 6: Shows the Correlation Results of the Five Cylinders in a Staggered Array with Cylinders Separating Distances  $S_T$  and  $S_L$  of  $2.5335 D$  and  $5 D$ , Respectively

Cylinders $P_0, P_3$ And $P_1$		Cylinders $P_4$ And $P_2$	
$\Theta$	Formula	$\Theta$	Formula
0	$Nu_{L,D} = 0.4821 (Gr_{L,D} Pr)^{0.253}$	0	$Nu_{L,D} = 0.6242 (Gr_{L,D} Pr)^{0.246}$
30	$Nu_{L,D} = 0.4661 (Gr_{L,D} Pr)^{0.252}$	30	$Nu_{L,D} = 0.5630 (Gr_{L,D} Pr)^{0.249}$
45	$Nu_{L,D} = 0.4416 (Gr_{L,D} Pr)^{0.253}$	45	$Nu_{L,D} = 0.5692 (Gr_{L,D} Pr)^{0.248}$
60	$Nu_{L,D} = 0.4291 (Gr_{L,D} Pr)^{0.252}$	60	$Nu_{L,D} = 0.5507 (Gr_{L,D} Pr)^{0.247}$
90	$Nu_{L,D} = 0.4103 (Gr_{L,D} Pr)^{0.252}$	90	$Nu_{L,D} = 0.4093 (Gr_{L,D} Pr)^{0.251}$

Table 7: Variation of Correlation Parameter  $C$  and the Percentage Enhancement Related to Vertical Array with Array Orientation, for Staggered Cylinders Arrangement

$\Theta$ Degree	$C_{P_0}$ And $C_{P_3}$	(%) Percentage Enhancement	$C_{P_1}$	(%) Percentage Enhancement	$C_{P_2}$ And $C_{P_4}$	(%)Percentage Enhancement
0	0.4821	17.5	0.4820	17.47	0.6242	52.5
30	0.4661	13.6	0.4660	13.57	0.5630	37.55
45	0.4416	7.6	0.441	7.48	0.5690	39.0
60	0.4291	4.58	0.4290	4.56	0.5507	34.55
90	0.4103	0	0.4103	0	0.4093	0

